THE CHARGE DISTRIBUTIONS OF THE OXYGEN AND CALCIUM ISOTOPES

B.A. BROWN, S.E. MASSEN and P.E. HODGSON
Nuclear Physics Laboratory, Oxford, UK

Received 17 May 1979

A new method of calculating the charge distributions of isotopic sequences is described and applied to the oxygen and calcium isotopes. It is based on the method of summing the squares of single-particle wave functions of the occupied orbits, together with an iteration procedure to ensure the self-consistency of the neutron and proton distributions. The interactions between the core and valence nucleons are included, and configuration mixing may be taken into account by using shell-model orbit occupation probabilities.

The Hartree–Fock method is widely used to calculate nuclear charge and matter distributions, but suffers from the disadvantages that the effective interaction is not well known and also that it becomes increasingly difficult to justify away from closed shells [1]. The method based on the sum of the squares of single-particle wave functions in a Saxon–Woods potential, on the other hand, is able to give precision fits to experimental charge distributions but is not self-consistent and lacks a realistic prescription for treating nearby nuclei in a unified way [2]. We have therefore extended the latter method to include self-consistency and the interactions between the core and the valence nucleons, and have applied it to calculate the charge distributions of several isotopic sequences of nuclei.

Our calculations proceed in two stages: we first obtain the proton distribution for the core nucleus by the usual (non-self-consistent) Saxon–Woods parameterization and then we extend the calculations to include the neutrons and the valence nucleons.

We use a potential of the standard form

$$V_{\mathrm{p,n}}(r) = V_{\mathrm{coul}}(r) + V_{\mathrm{p,n}} f(r) + V_{\mathrm{so}}(r) , \qquad (1)$$

where $V_{\mathrm{coul}}(r)$ is the Coulomb potential that is present only for protons, $V_{\mathrm{p,n}} f(r)$ the central potential, $V_{\mathrm{so}}(r)$ the spin–orbit potential and

$$f(r) = [1 + \exp\{(r - R)/a\}]^{-1} .$$

Instead of the usual expression

$$V_{\mathrm{p,n}} = V_0 \pm ((N - Z)/A) V_1 , \qquad (2)$$

we use

$$V_{\mathrm{p,n}} = V_0 \pm (\rho_1(r)/\rho_0(r)) V_1 , \qquad (3)$$

where

$$\rho_0 = \rho_{\mathrm{n}}(r) + \rho_{\mathrm{p}}(r) , \qquad (4)$$

and

$$\rho_1 = \rho_{\mathrm{n}}(r) - \rho_{\mathrm{p}}(r) ,$$

where $\rho_{\mathrm{n}}(r)$ and $\rho_{\mathrm{p}}(r)$ are the neutron and proton distributions, respectively. Unlike eq. (2) the isospin term in form (3) is non-zero for $N = Z$ nuclei, and so enables the difference between the two distributions for these nuclei to be calculated self-consistently.

We begin by adjusting the parameters V_0 and R to give the rms charge radius of a closed-shell (core) nucleus, and the experimental *proton* single-particle centroid energies. The neutron and proton distributions are defined by expressions of the form

$$\rho(r) = \frac{1}{4\pi} \sum n(nlj) \left| \frac{1}{r} U_{nlj}(r) \right|^2 , \qquad (5)$$

where the $n(nlj)$ are occupation probabilities, $U_{nlj}(r)$ the radial wave functions and the sum runs over all occupied orbits. The symmetry potential $V_1 = 30$ MeV and the other parameters have standard values $V_{\mathrm{so}} = 7$ MeV, $a = 0.65$ fm, $a_{\mathrm{so}} = 0.65$ fm, and $R_{\mathrm{so}} = 1.1A^{1/3}$ fm.

After the first calculation, the proton and neutron distributions are inserted in eq. (3) and the whole calculation iterated to self-consistency in the proton and neutron distributions. To obtain the charge and matter distributions these are folded with the corresponding distributions of the nucleons themselves, and the spin–orbit, Darwin–Foldy and centre-of-mass motion corrections are included in the usual way.

To extend the calculation to nuclei with valence nucleons, the central potential is written in the form

$$V_{p,n}f(r) = \{V_0\,\rho_0(r) \pm V_1\,\rho_1(r)\}F(r)\,, \qquad (6)$$

where $F(r) = f(r)/\rho_0^c(r)$, and $\rho_0^c(r)$ refers to the core nucleus. This expression is identical to eq. (3) for the core nucleus but for nuclei with valence nucleons it has additional terms that include the effects of the interaction between the core and valence nucleons.

Using this potential, the calculation can then be repeated for the nuclei in an isotopic sequence without any additional parameters. Throughout the calculation the potentials are constrained to fit the single-particle centroid energies and the orbit occupation probabilities are taken either from analyses of nucleon transfer reactions or from shell-model calculations.

In contrast to previous calculations [2], we have made no attempt to adjust the Saxon–Woods parameters or occupation probabilities in order to fit the details of the radial dependence (the oscillations) of the total charge distribution of the closed shell nuclei. This is because these details are probably very sensitive to short range aspects of the nuclear force which are not included in the non-self-consistent Saxon–Woods potential and in addition mesonic effects which are not included and are difficult to calculate may give rise to additional effective oscillations in the charge density. Rather, we concentrate here on the charge density differences between different members of the isotope which give a direct measure of the rearrangement of charge due to core-polarization and shell-breaking effects.

This method has been applied to the oxygen and calcium isotopes, and some of the results are shown in figs. 1–3. In the case of oxygen, we calculate the charge distribution differences (1) with the simple model of one or two neutrons outside a closed ^{16}O core and (2) using the Reehal–Wildenthal [3] interaction within a model space of $1p_{1/2}$, $2s_{1/2}$ and $1d_{5/2}$ (psd) allowing for up to four holes in the $p_{1/2}$ orbit.

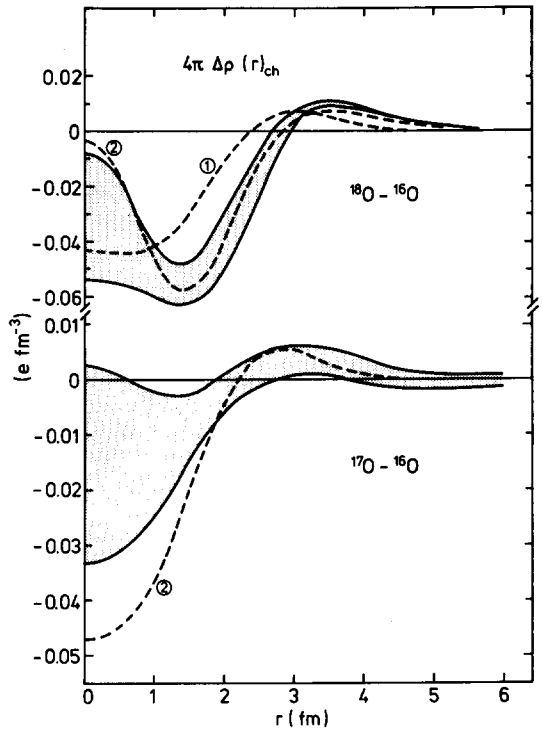

Fig. 1. Experimental charge density differences between ^{17}O and ^{16}O and between ^{18}O and ^{16}O (Miska et al. [6]) compared with calculations using (1) closed 1s and 1p shell configurations, and (2) the occupation probabilities from the Reehal–Wildenthal wave functions.

In (1) we take valence configurations with one neutron in the $1d_{5/2}$ orbit for ^{17}O and an $(sd)^2$ configuration for ^{18}O with occupation probabilities calculated with the Chung–Wildenthal [4] interaction. The psd occupation probabilities of ^{18}O and ^{17}O relative to ^{16}O, which are the quantities relevant to the change in the charge distribution, are given by $\Delta n_p(p) = -0.05$, $\Delta n_p(d) = 0.04$, $\Delta n_p(s) = 0.01$, $\Delta n_n(p) = 0.000$, $\Delta n_n(d) = 0.99$ and $\Delta n_n(s) = 0.01$ for ^{17}O–^{16}O, $\Delta n_p(p) = 0.49$, $\Delta n_p(d) = 0.31$, $\Delta n_p(s) = 0.18$, $\Delta n_n(p) = -0.21$, $\Delta n_n(d) = 1.77$ and $\Delta n_n(s) = 0.44$ for ^{18}O–^{16}O. The psd occupation difference between ^{17}O and ^{16}O is well represented by a $d_{5/2}$ neutron weakly coupled to ^{16}O and hence the calculations (1) and (2) are essentially identical in this case; only (2) is shown in fig. 1.

The desirability of using wave functions with 6p–4h excitations for ^{18}O is shown by comparing the rms charge radii with those obtained with a simpler one-

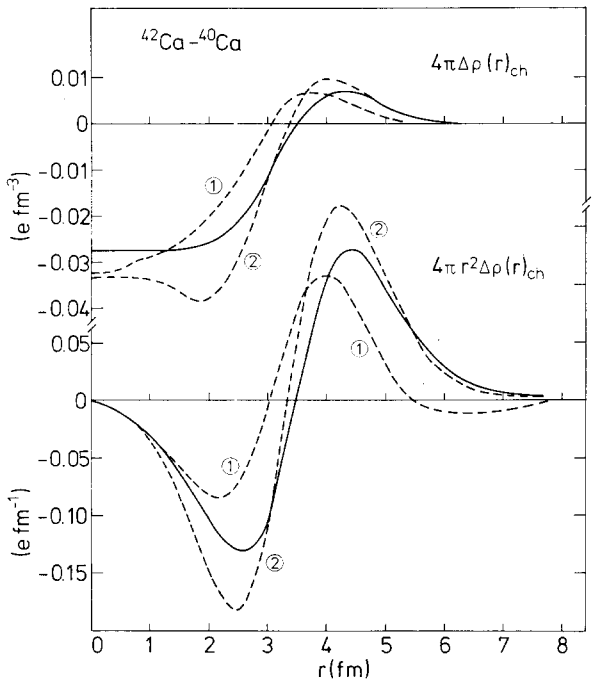

Fig. 2. Experimental and theoretical charge density differences between ^{42}Ca and ^{40}Ca. The experimental curve is from the model-dependent fit to the electron scattering data by Frosch et al. [11]. The two theoretical curves correspond to (1) a closed sd shell configuration, and (2) a non-closed sd shell configuration with $\Delta(2) = 1.0$.

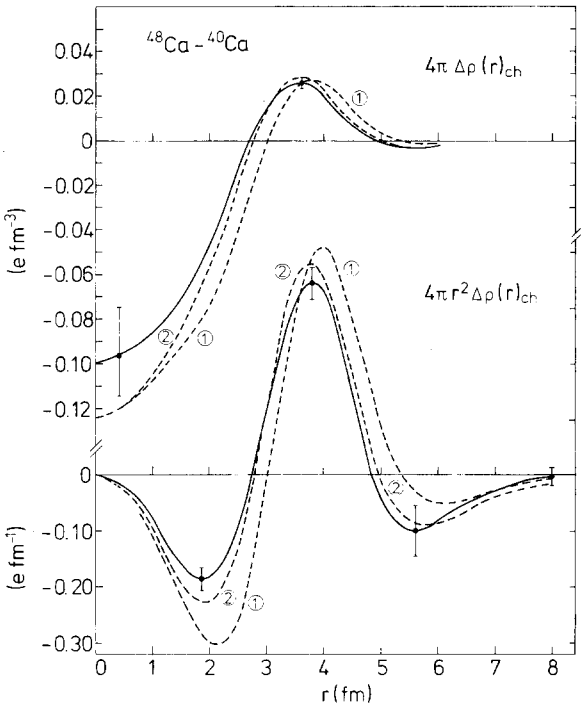

Fig. 3. Experimental and theoretical charge density differences between ^{48}Ca and ^{40}Ca. The experimental curve is from the model-independent fits of Sick [12] and Frois [16] and the theoretical curves correspond to (1) a closed sd shell configuration, and (2) a non-closed sd shell configuration with $\Delta(8) = -0.4$.

parameter schematic wave function of the form

$$|^{18}O\rangle = \alpha|(\nu sd)^2\rangle + \beta|(\pi p_{1/2})^{-2}(\pi sd)^2(\nu sd)^2\rangle\,, \qquad (7)$$

which has been used by Lawson et al. [5]. To reproduce the experimental rms charge radius with this simplified wave function we need $\beta^2 = 0.20$, implying 0.39 fewer p-shell protons in ^{18}O than in ^{16}O. However, this value of β^2 is inconsistent with the analyses of other data such as B(E2) values and spectroscopic factors which give $\beta^2 = 0.10$ [5]. This probably indicates the need for including 6p–4h excitations. The psd wave functions which include such configurations gives 0.073 fm for the difference in rms radii between ^{16}O and ^{18}O, in agreement with the experimental value of 0.074 ± 0.005 [6]. The corresponding values for ^{17}O are 0.003 fm compared with -0.008 ± 0.007 fm [4]. The experimental and theoretical values of the rms radii themselves are compared in table 1.

Many previous calculations have been made for the calcium isotopes using the Saxon–Woods [7] and Hartree–Fock [8] methods. Compared with the present calculations the former have too many parameters

Table 1
Rms charge radii.

Experiment a)		Theory	
		(1)	(2)
^{16}O	2.720 (4)	2.720	2.720
^{17}O	2.712 (5)	2.726	2.723
^{18}O	2.794 (3)	2.730	2.793
^{40}Ca	3.480	3.483	3.476
^{42}Ca	3.510	3.490	3.510
^{44}Ca	3.520	3.497	3.515
^{46}Ca	3.501	3.503	3.493
^{48}Ca	3.481	3.509	3.473

a) The experimental data are from refs. [6] and [15] for the oxygen and calcium isotopes, respectively.

while the latter are not in good accord with experiment, probably due to the neglect of non-closed shell configurations.

In our calculations we first assume a closed sd shell with valence neutrons in the fp shell, and use simplified but realistic fp shell occupation probabilities of 90% $1f_{7/2}$ particles plus 10% $2p_{3/2}$ particles. The resulting isotopic dependence of the rms radii given in table 1 is weak and smooth in disagreement with experiment, but the density changes are large and in qualitative agreement with experiment as shown in figs. 2 and 3.

The amount of proton excitation from the sd shell to the fp shell needed to reproduce the rms radii was then determined using the following wave functions, for $n \geqslant 2$:

$$|^{40+n}\mathrm{Ca}\rangle = \alpha|(\nu f_{7/2}p_{3/2})^n\rangle + \beta|(\pi d_{3/2})^{-2}(\pi f_{7/2}p_{3/2})^2(\nu f_{7/2}p_{3/2})^n\rangle , \quad (8)$$

and

$$|^{40}\mathrm{Ca}\rangle = \alpha|0\rangle + \beta|(\pi d_{3/2})^{-1}(\pi f_{7/2}p_{3/2}) \times (\nu d_{3/2})^{-1}(\nu f_{7/2}p_{3/2})\rangle , \quad (9)$$

where $|0\rangle$ is the closed shell configuration and it is assumed that the $f_{7/2}p_{3/2}$ configuration is as before. The number of proton holes in the $d_{3/2}$ orbit relative to ^{40}Ca is given by

$$\Delta(n) = 2\beta^2(^{40+n}\mathrm{Ca}) - \beta^2(^{40}\mathrm{Ca}) . \quad (10)$$

We have rather arbitrarily chosen a value of $\beta^2(^{40}\mathrm{Ca}) = 0.7$ and have adjusted R to reproduce the ^{40}Ca rms charge radius. The value of β^2 which we use for ^{40}Ca and those which we will find for the other calcium isotopes are unrealistically large in order to compensate for the many-particle many-hole parts of the wave function which are not explicitly included.

The quantity $\Delta(n)$ was fixed to reproduce the isotopic dependence of the experimental rms radii; this gives $\Delta(2) = 1.0$, $\Delta(4) = 1.1$, $\Delta(6) = 0.35$ and $\Delta(8) = -0.4$. The results of these calculations are compared with the experimental charge distribution differences in figs. 2 and 3. On the whole the agreement is excellent. The calculation (2) which includes core excitation is much better than the closed shell calculation (1) especially in the surface region. We note that the experimental curve for ^{42}Ca–^{40}Ca shown in fig. 2 from ref. [11] is very model dependent; new data and a model-independent fit for the ^{42}Ca electron scattering is essential. The experimental and theoretical rms charge radii are compared in table 1.

The values of Δ obtained in this way from electron scattering are compared in table 2 with the estimates of the numbers of proton holes in the sd shell H(sd) obtained from analyses of stripping reactions and from the particles in the fp shell P(fp) from pickup reactions. Consistency then requires $\Delta + \delta = P(\mathrm{fp}) = H(\mathrm{sd})$ where δ is the number of proton holes in ^{40}Ca; we have arbitrarily chosen $\delta = 0.7$ for our calculations. Examination of table 1 shows that none of these quantities agree well. The discrepancy between the stripping and pickup reactions has already been noted [10] and is probably connected with the need to include all high-lying states and to take account of the anomalies that arise when comparing states of very different binding energies [13].

Many shell model calculations of increasing sophistication have been made for the calcium isotopes [14], but they are still far from explaining the experimental situation. In particular, the values of Δ are in very poor agreement with theory except in the case of the large-basis calculations for ^{40}Ca including configurations up to 4p–4h and 8p–8h.

This model is thus able to account for many features of the charge distributions of the oxygen and calcium isotopes. It is in several respects complementary to the Hartree–Fock method, as it takes full account of the complex configuration mixing in light nuclei but is not fully self-consistent as the potential is allowed to vary only linearly with the density. The Hartree–Fock

Table 2
Comparison of the number of proton holes in the sd shell obtained from electron scattering ($\Delta + \delta$), pickup reactions [P(fp)], and stripping reactions [H(sd)].

	$\Delta + \delta$	H(sd) [a]	H(sd) [b]	P(fp) [c]	P(fp) [d]
^{40}Ca	0.7	0.4	0.27	0.73	0.3
^{42}Ca	1.7	0.9	1.12	1.03	0.4
^{44}Ca	1.8	1.9	1.98	1.01	0.6
^{46}Ca	1.05	0.4			0.2
^{48}Ca	0.3	0.15	0.44	0	0

a) (^{3}He, d), quoted by v.d. Decken et al. [9]. b) (^{3}He, d), quoted by Doll et al. [10]. c) (d, ^{3}He), Doll et al. [10]. d) (t, α), quoted by Dehnhard and Cage [17].

method, on the other hand, is fully self-consistent but the configuration is restricted to a single Slater determinant with the particles in the lowest spherical or deformed configuration.

Once the parameters of this model are fixed by comparison with the charge distributions it gives the neutron distributions without further parameter adjustment. The comparison of the resulting distributions with the experimental data will be reported separately.

References

[1] J.W. Negele, Proc. Conf. on Modern trends in elastic electron scattering (Amsterdam, 1978) p. 73.
[2] F. Malaguti, A. Uguzzoni, E. Verondini and P.E. Hodgson, Nucl. Phys. A297 (1978) 287.
[3] B.S. Reehal and B.H. Wildenthal, Part. Nucl. 6 (1973) 137.
[4] W. Chung and B.H. Wildenthal, to be published (1978).
[5] R.L. Lawson, F.J.D. Serduke and H.T. Fortune, Phys. Rev. C14 (1976) 1245.
[6] M. Miska, B. Norvm, M.W. Hynes, W. Bertozzi, S. Kowalski, F.N. Rad, C.P. Sargent, T. Sasanuma and B.L. Berman, preprint (1978).
[7] B.F. Gibson and K.J. Van Oostrum, Nucl. Phys. A90 (1967) 159;
L.R.B. Elton, Phys. Rev. 158 (1967) 970;
L.R.B. Elton and S.J. Webb, Phys. Rev. Lett. 24 (1970) 145;
F. Malaguti, A. Uguzzoni, E. Verondini and P.E. Hodgson, Nuovo Cimento 49A (1979) 412.
[8] J.W. Negele, Phys. Rev. C1 (1970) 1260;
W. Bertozzi, J. Friar, J. Heisenberg and J.W. Negele, Phys. Lett. 41B (1972) 408.
[9] A.v.d. Decken et al., Phys. Lett. 41B (1972) 477.
[10] P. Doll, G.J. Wagner, K.T. Knöpfle and G. Mairle, Nucl. Phys. A263 (1976) 210.
[11] R.F. Frosch et al., Phys. Rev. 174 (1968) 1380.
[12] I. Sick, Phys. Lett. 53B (1974) 15; private communication (1978).
[13] A. Moalem, J.F.A. van Hienen and E. Kashy, Nucl. Phys. A307 (1978) 277.
[14] W.J. Gerace and A.M. Green, Nucl. Phys. A93 (1967) 110; A123 (1969) 241;
K.K. Seth et al., Phys. Rev. Lett. 33 (1974) 233;
P. Federman and S. Pittel, Phys. Rev. 186 (1969) 1106;
M. Sakakura, A. Arima and T. Sebe, Phys. Lett. 61B (1976) 335.
[15] H.D. Wohlfahrt et al., Phys. Lett. 73B (1978) 131.
[16] B. Frois, Proc. Conf. on Modern trends in elastic electron scattering (Amsterdam, 1978) 1.
[17] D. Dehnhard and M.E. Cage, Nucl. Phys. A230 (1974) 393.